NASA/TM—2015-218884

# Hot Isostatic Pressing of 60-Nitinol

*Malcolm K. Stanford*
*Glenn Research Center, Cleveland, Ohio*

October 2015

# NASA STI Program . . . in Profile

Since its founding, NASA has been dedicated to the advancement of aeronautics and space science. The NASA Scientific and Technical Information (STI) Program plays a key part in helping NASA maintain this important role.

The NASA STI Program operates under the auspices of the Agency Chief Information Officer. It collects, organizes, provides for archiving, and disseminates NASA's STI. The NASA STI Program provides access to the NASA Technical Report Server—Registered (NTRS Reg) and NASA Technical Report Server—Public (NTRS)  thus providing one of the largest collections of aeronautical and space science STI in the world. Results are published in both non-NASA channels and by NASA in the NASA STI Report Series, which includes the following report types:

- TECHNICAL PUBLICATION. Reports of completed research or a major significant phase of research that present the results of NASA programs and include extensive data or theoretical analysis. Includes compilations of significant scientific and technical data and information deemed to be of continuing reference value. NASA counter-part of peer-reviewed formal professional papers, but has less stringent limitations on manuscript length and extent of graphic presentations.

- TECHNICAL MEMORANDUM. Scientific and technical findings that are preliminary or of specialized interest, e.g., "quick-release" reports, working papers, and bibliographies that contain minimal annotation. Does not contain extensive analysis.

- CONTRACTOR REPORT. Scientific and technical findings by NASA-sponsored contractors and grantees.

- CONFERENCE PUBLICATION. Collected papers from scientific and technical conferences, symposia, seminars, or other meetings sponsored or co-sponsored by NASA.

- SPECIAL PUBLICATION. Scientific, technical, or historical information from NASA programs, projects, and missions, often concerned with subjects having substantial public interest.

- TECHNICAL TRANSLATION. English-language translations of foreign scientific and technical material pertinent to NASA's mission.

For more information about the NASA STI program, see the following:

- Access the NASA STI program home page at http://www.sti.nasa.gov

- E-mail your question to help@sti.nasa.gov

- Fax your question to the NASA STI Information Desk at 757-864-6500

- Telephone the NASA STI Information Desk at 757-864-9658

- Write to:
  NASA STI Program
  Mail Stop 148
  NASA Langley Research Center
  Hampton, VA 23681-2199

# Hot Isostatic Pressing of 60-Nitinol

*Malcolm K. Stanford*
*Glenn Research Center, Cleveland, Ohio*

National Aeronautics and
Space Administration

Glenn Research Center
Cleveland, Ohio 44135

October 2015

## Acknowledgments

# Hot Isostatic Pressing of 60-Nitinol

Malcolm K. Stanford
National Aeronautics and Space Administration
Glenn Research Center
Cleveland, Ohio 44135

## Abstract

The effects of varying the time, temperature and pressure during consolidation of 60-NITINOL by hot isostatic pressing (HIP) were examined. Six HIP cycles with a cycle time of either 2 or 20 h, temperature of 900 or 1000 °C, and a chamber pressure of either 100 or 200 MPa were used. The cycle representing the shortest cycle time at the highest temperature and pressure (2 h/1000 °C/200 MPa) produced material with the highest hardness (720 HV). A modest increase in average grain size and significant porosity reduction were observed in material subjected to the longest cycle time at the highest temperature, regardless of the pressure applied. The intent of this study is to facilitate the technology transfer involved in the processing of this material.

## Introduction

60-Nitinol (60wt%Ni – 40wt%Ti) has a unique combination of physical properties, including high hardness, low apparent elastic modulus and resistance to saltwater corrosion (Ref. 1). These properties give the material tremendous potential for use in aerospace and defense-related components such as bearings, gears and other apparatuses (Refs. 2 to 4). Various methods of primary processing are being explored for fabrication of high-performance components that are free of metallurgical defects that might lead to premature failure. Hot isostatic pressing, herein abbreviated HIP, is one process under consideration. As shown schematically in Figure 1, the steps in the HIP process include (a) filling a sealed canister of the appropriate dimensions with powder, (b) heating the canister under vacuum to remove volatile and gaseous contents, (c) applying heat and pressure to the evacuated and sealed canister to consolidate the contents and (d) removal of the canister (Ref. 5).

When used to consolidate metal powders, HIP has distinct advantages over other processing techniques such as casting (Ref. 5). Namely, the mechanical properties of the consolidated material tend to be more isotropic due to the random orientation of grains, which are dictated by the random orientation of the powder particles. Likewise, the bulk material tends to be more chemically homogeneous due to reduced chemical segregation. Also, the defect size within the bulk material tends to approximate the particle size. One of the major disadvantages of HIP is the cost. The purchase cost of the powders, HIP processing (especially if long cycle times are needed) and canister removal can represent a barrier to technological development and adoption by industry. In addition, due to the fact that hydrostatic forces are applied during consolidation, there are no shear forces that might otherwise act to disrupt adsorbed oxide films on particles (Ref. 5). These oxide films then persist in the bulk material, serving as potential fracture propagation paths, as was discovered in previous work in the author's laboratory (Ref. 6). During development efforts of 60-Nitinol at NASA Glenn Research Center, high porosity and unconsolidated particles were observed in 60-Nitinol that was prepared by HIP (Refs. 6 and 7). Figures 2 and 3 shows some examples. These unconsolidated particles were found to be the result of oxidized particles in the powder and were found to play a role in fracture initiation during fracture energy tests. It was unclear whether the HIP cycle could be further optimized, so a study was initiated to determine the effects of the HIP processing parameters of time, temperature and pressure on the consolidation of 60-Nitinol.
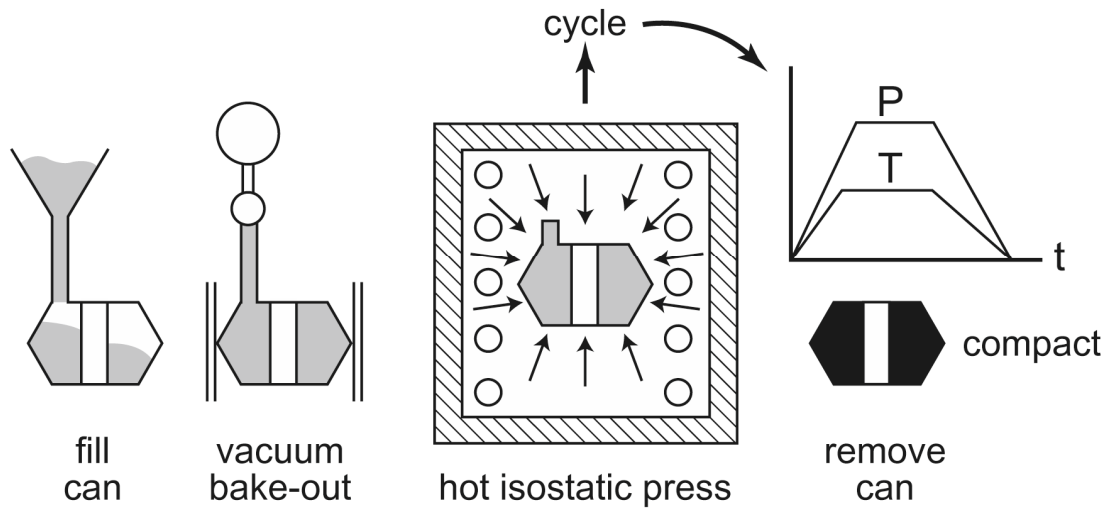
Figure 1.—Schematic depiction of the steps involved in HIP (Ref. 5).
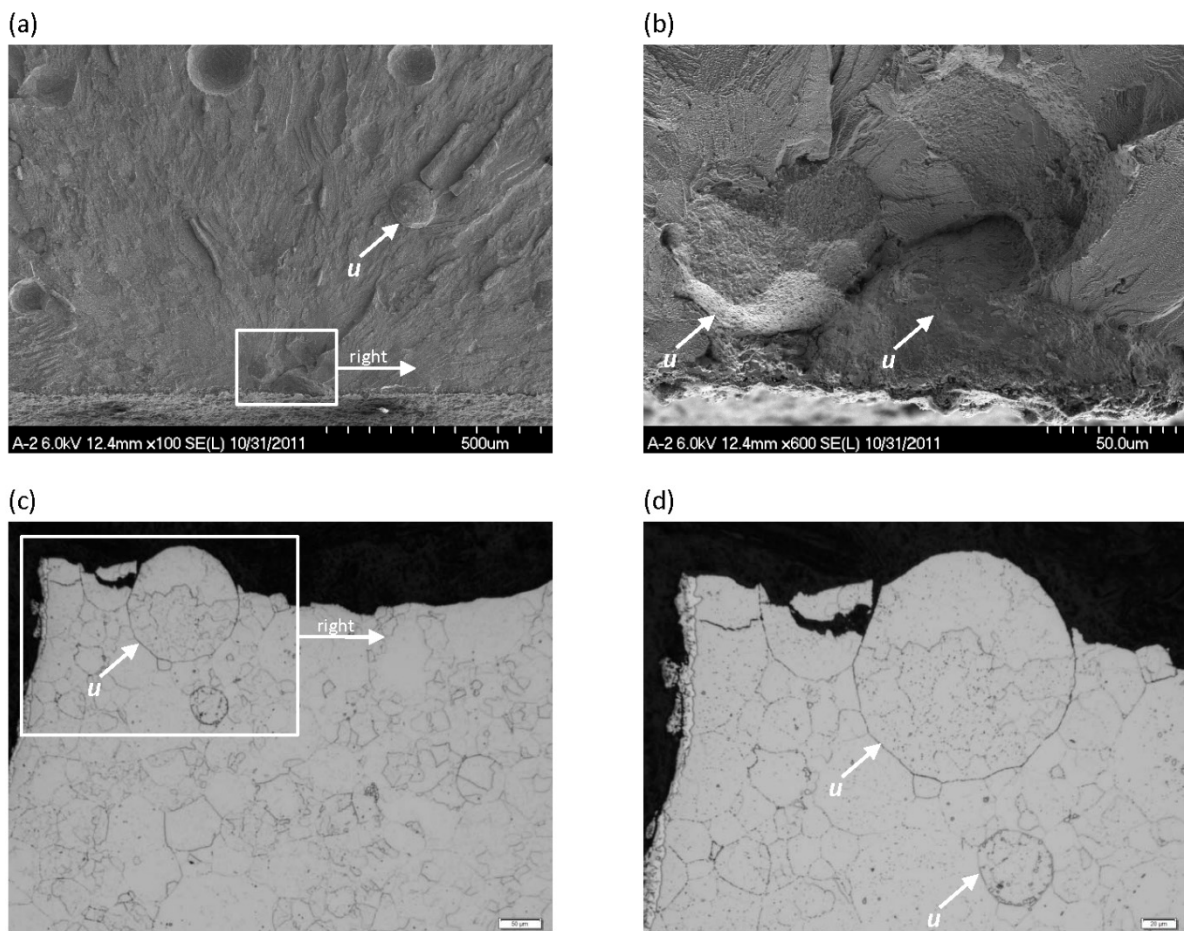


Figure 2.—An FESEM image of a fracture surface is shown in (a) with unconsolidated particles **u**, as well as depressions that mark the previous locations of unconsolidated particles. A higher-magnification image of the fracture initiation site (b) also shows unconsolidated particles. A cross section of this specimen also shows unconsolidated particles **u** (c) and a higher-magnification view (d) (Ref. 6).
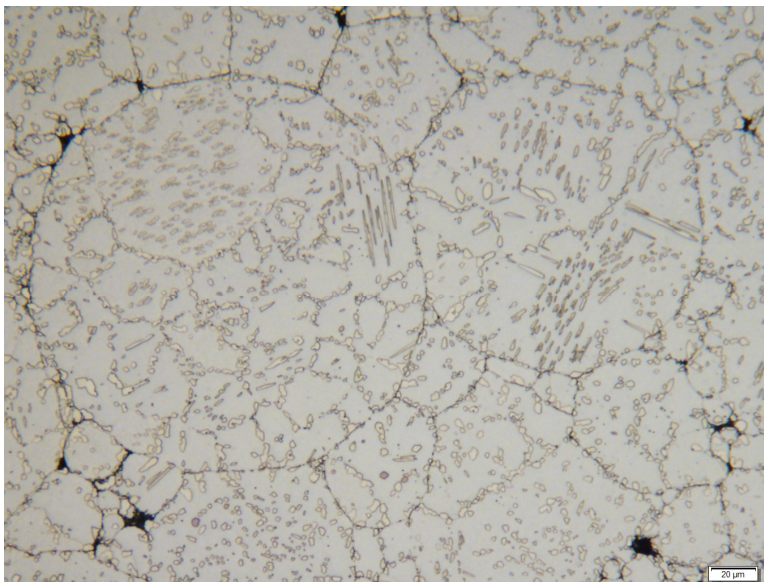
Figure 3.—Photomicrograph of baseline 60-Nitinol showing incomplete consolidation as evidenced by high levels of angular porosity and unconsolidated particles (Ref. 5). This specimen was heat treated at 1,000 °C then furnace cooled. The polished cross section was etched with an aqueous 1vol%HF-10vol%HNO$_3$ solution.

## Experimental Procedures

A –60 mesh sieve fraction of gas atomized 60-Nitinol powder was obtained from a commercial source. The chemical composition of this powder was analyzed by inductively-coupled plasma atomic emission spectroscopy (ICP-AES) (Refs. 8 and 9). The crystalline phases were identified by x-ray diffraction (XRD) using Cu K$\alpha$ radiation. A sample of the powder was dried for an hour at approximately 100 °C under a moderate vacuum. Particle size was measured using the light-scattering technique (Ref. 10). Powder density and flow rate were measured using standard test specifications (Refs. 11 to 13). Photomicrographs of the feedstock powder are shown in Figures 4 and 5. The equiaxed grain structure visible on the particle surfaces as well as on the cross-sections indicate a cooling rate consistent with inert gas atomization (Ref. 14). In Figure 3, an approximately 20 μm "satellite" particle can be seen attached to an approximately 150 μm particle. This was the result of a collision between the two particles before they completely solidified during the atomization process. Some of the particles have hollow regions, which are a result of the dissolution of gasses as the molten material cooled (Refs. 15 and 16).

A baseline comparison was made to a specimen from the same lot of powder HIP-consolidated by a commercial vendor using a business-sensitive process. The specimen was heat treated for 2 h at 1050 °C, water quenched and then ground to render a bright metal surface, removing surface oxides from heat treating. The chemical composition and crystalline phases present in this consolidated material were determined by ICP-AES and x-ray diffraction as with the powder precursor material mentioned previously. A helium pycnometer with typical reproducibility within 0.01 percent of the nominal full-scale sample cell chamber volume was used to measure the skeletal volume of the specimen, following a standard procedure (Ref. 17). The weight of the specimen was measured using an analytical balance with 0.002 mg readability. The volumetric density of the specimen was then calculated using the average of 5 skeletal volume measurements and the average of ten weight measurements. Standard metallographic procedures were used to prepare the specimen for microscopy, starting with rough grinding using a 220 grit resin bonded diamond grinding disc at 300 rpm and 150N and concluding with vibratory polishing with 0.01 μm colloidal silica (Ref. 18). Microindentation hardness was measured on this specimen using a 200 gf load and a 15 sec load application according to a standard test method (Ref. 19).

a.



b.
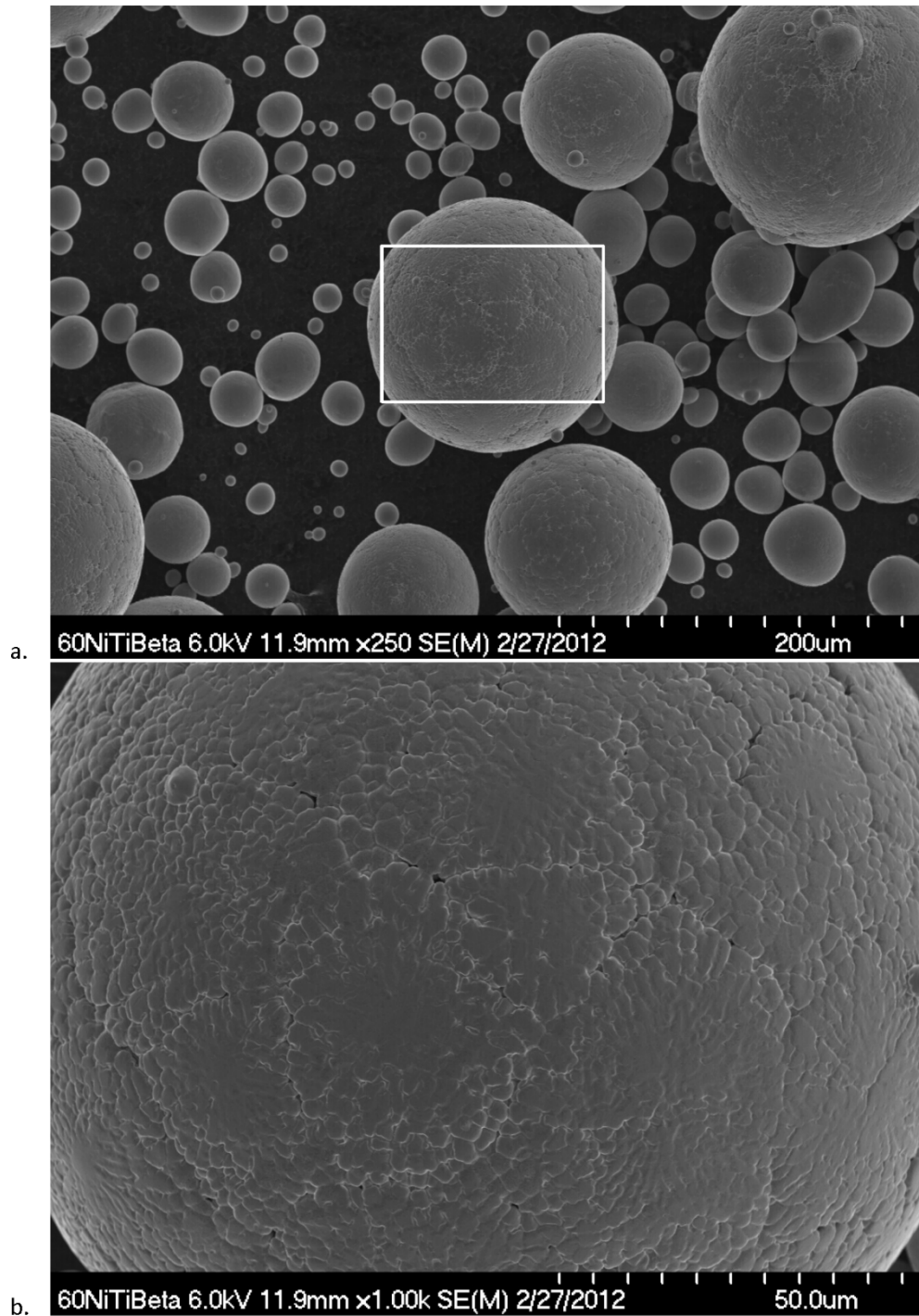
Figure 4.—(a) FESEM images of the starting powder showing spherical particle morphology (b) and an equiaxed grain structure on the surface.
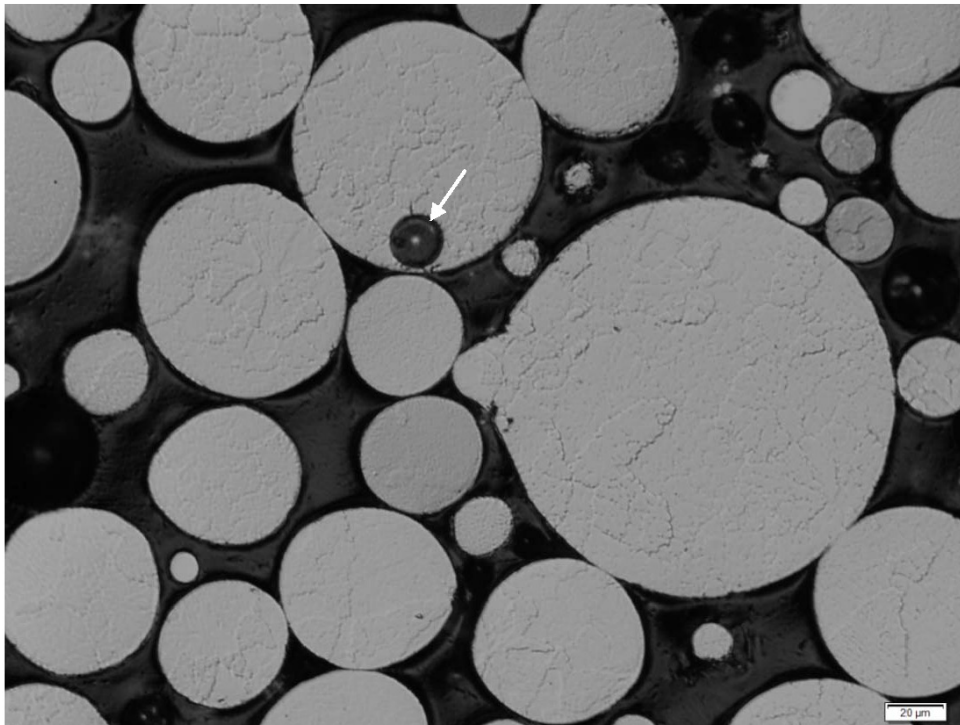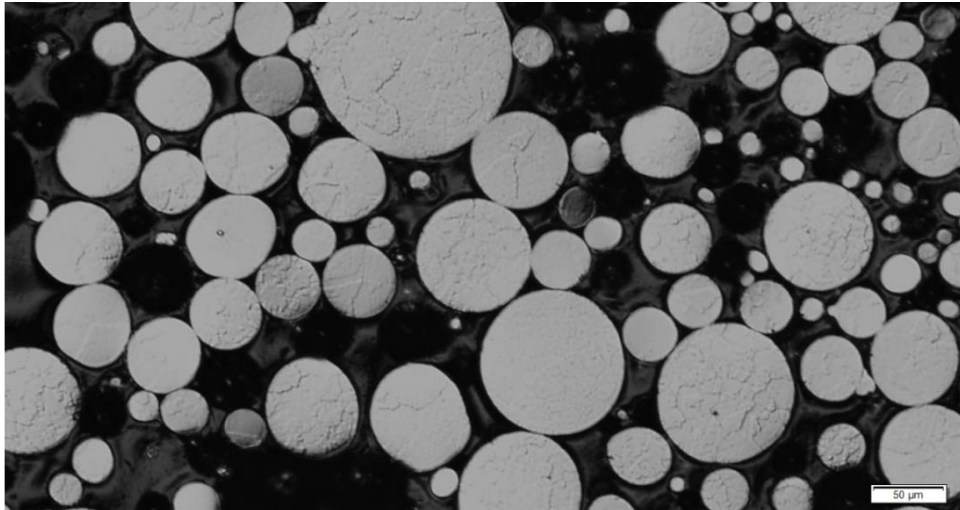
Figure 5.—Differential interference contrast optical photomicrographs of cross-sectioned powder particles, swab-etched with a room temperature aqueous solution of 1vol%Hf and 10vol%HNO$_3$. A particle near the top center of the bottom photomicrograph has a hollow region (indicated with an arrow) that formed as a result of trapped gas during particle fabrication.

Six steel canisters, each approximately 63 mm in diameter by 102 mm long were filled with powder, degassed and individually sealed under vacuum. The material was consolidated by HIP in nitrogen using one of the six cycles listed in Table 1. The HIP cycles were selected to represent a combination of the highest and lowest practical settings for each parameter under consideration, based on previous HIP runs for this material. This study was originally intended to produce data for a three-factor design of experiments with two levels. However, two canisters were damaged during setup and processing and could not be used. It was hoped that the remaining specimens would generate sufficient data to provide indications for process improvements. A 20 mm diameter cylinder was cored out of the center of each consolidated specimen. Figure 6 shows a canister after consolidation, with the core removed. From the core, a 5 mm thick disk was cut from the center. Each specimen disk was cut in half, and one half was heat treated in vacuum at 1050 °C for 2 h followed by water-quenching. This heat treatment, designated the *water-quench* (*WQ*), is designed to precipitation harden the material. Both the water-quenched and the as-HIPped halves of each specimen were mounted in Bakelite and prepared for hardness testing and microstructural examination of the mating surfaces.

TABLE 1.—HOT ISOSTATIC
PRESSING PARAMETERS

| HIP cycle identifier | Parameters |
|---|---|
| A | 2 h/900 °C/200 MPa |
| B | 2 h/1000 °C/100 MPa |
| C | 2 h/1000 °C/200 MPa |
| D | 20 h/900 °C/100 MPa |
| E | 20 h/1000 °C/100 MPa |
| F | 20 h/1000 °C/200 MPa |



Figure 6.—HIP can with cylinder of
material removed by wire electrical
discharge machining after consolidation.

Microindentation hardness testing was performed using the procedure previously cited. A linear indentation spacing of 500 μm was used to prevent near-field strain-hardening, which could induce increasing hardness on adjacent indentations. No attempt was made to select the location of indentations with respect to precipitate phases or grain boundaries. The average and standard deviation of five hardness measurements was reported for each specimen.

Microstructural analysis was performed on the studied material using optical microscopy and field-emission scanning electron microscopy (FESEM). Commercially-available image analysis software was used to capture and process microstructural images. The procedure was to first correct for lens effects such as gradients. Appropriate thresholds for discrimination between white second phase $Ni_3Ti$, grey NiTi parent phase and black porosity were selected based upon the spectral histogram. The images were calibrated. Each pixel corresponded to approximately 0.5 μm both vertically and horizontally. Each monochromatic photomicrograph had a bit-depth of 8 bits per pixel with an image size of 1,360 by 1,024 pixels. Thirty-five images were captured for each specimen at a magnification of 200 times. They cover an area of approximately $3.3 \times 10^6$ $\mu m^2$ per specimen. This technique did not account for the morphology or size distribution of the detected second phase or pores. Grain size was measured using the planimetric method (Ref. 20).

# Results and Discussion

Physical properties of the powder are listed in Table 2. The powder consisted of NiTi and $Ni_4Ti_3$ phases and was free-flowing, as evidenced by its relatively low Hall flow time. The flowability of this powder was partially a result of its spherical shape, which results in low interparticle friction (Refs. 5 and 21). Another indication of the free-flowing nature of this powder was found by dividing the tap density (4.60 $g/cm^3$) by the apparent density (4.13 $g/cm^3$), which gives a value of 1.1. A value close to unity (as found for this powder) is another indication of a free-flowing powder that will easily fill a HIP canister, especially when flowing into tight fillets and radiuses (Refs. 5, 22, and 23).

Photomicrographs of the baseline material before and after heat treatment are shown in Figure 7. The etching technique was generally successful at revealing the grain boundaries, many of which are also prior particle boundaries. It is suspected that some of the well-defined prior particle boundaries (Fig. 7) could also be evidence of incomplete consolidation. Table 3 gives physical characteristics of the baseline material. The difference in chemical composition before and after consolidation is negligible within the expected experimental error.

TABLE 2.—POWDER CHARACTERIZATION DATA FOR
FEEDSTOCK POWDER USED IN THIS STUDY

| | |
|---|---|
| Nominal composition | 59.7wt%Ni – 40.2wt%Ti |
| Impurities (ppm) | O (730), Al (400), Fe (120), C (200), N (15) |
| Crystalline phases | Cubic NiTi and rhombohedral $Ni_4Ti_3$ |
| Feedstock sieve fraction | –60 mesh (<250 μm) |
| Particle size data | $D_{mean} = 123.8 \pm 60.5$ μm<br>$D_5 = 40.7$ μm<br>$D_{10} = 49.2$ μm<br>$D_{50}$ (median) = 129.4 μm<br>$D_{90} = 192.2$ μm<br>$D_{95} = 208.9$ μm |
| Apparent density | 4.13±0.01 $g/cm^3$ |
| Tap density | 4.60±0.04 $g/cm^3$ |
| Hall flow time (50 g sample) | 12.6±0.1 sec |
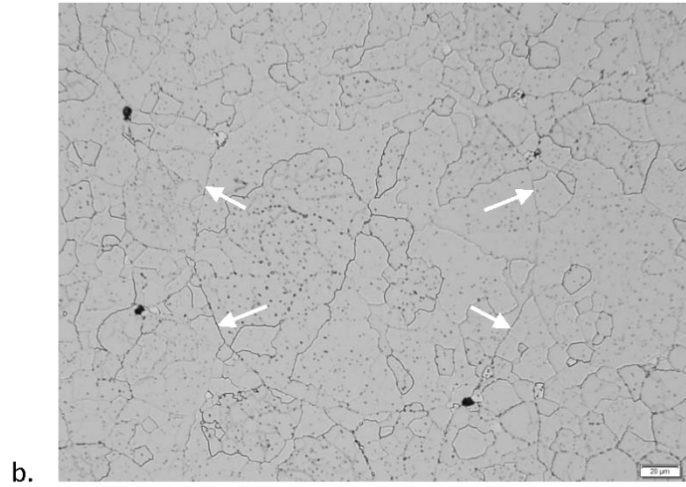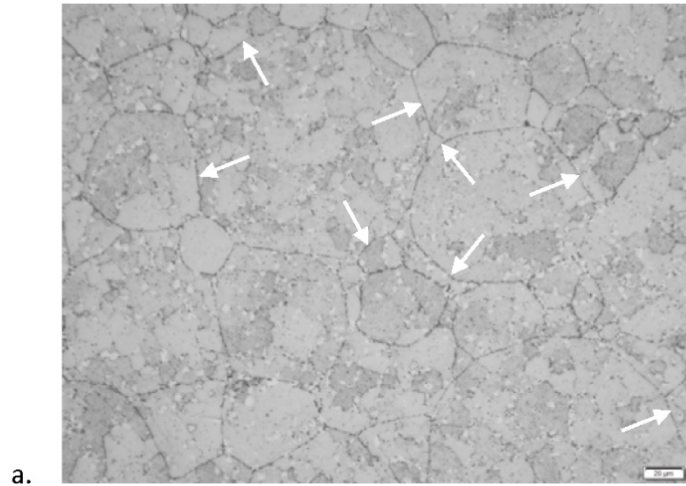
Figure 7.—Optical photomicrographs of the baseline material (a) after HIP and (b) after heat treatment, swab-etched with a room temperature aqueous solution of 1vol%Hf and 10vol%HNO$_3$. Several prior particle boundaries, which may indicate incomplete consolidation, are pointed out with arrows.

TABLE 3.—BASELINE PHYSICAL CHARACTERISTICS OF THE SUPPLIER-CONSOLIDATED MATERIAL

| | |
|---|---|
| Nominal composition | 59.6wt%Ni – 40.3wt%Ti |
| Impurities (ppm) | O (680), Al (200), Fe (130), C (210), N (40), Mn (4) |
| Crystalline phases | Cubic and monoclinic NiTi, hexagonal Ni$_3$Ti and rhombohedral Ni$_4$Ti$_3$ |
| Density | 6.66 g/cm$^3$ |
| Porosity | 0.2% |
| Microindentation hardness: (heat treated 2 h at 1050 °C then water-quenched): | 668.5±18.1 HV |

Figure 8 shows photomicrographs of material that underwent the two-hour HIP cycles A, B and C and was subsequently heat treated. Some pores remain at the interstices of several particles or as a remnant of trapped gas within a particle. Because there was slight variation in the revelation of grain boundaries in Figures 8(a), (c) and (e), the differential interference contrast photomicrographs shown in Figures 8(b), (d), and (f) helped to emphasize the grain boundaries for better comparison. The prior particle boundaries observed after HIP cycles A and B (Figs. 8(a) and (b)) are well-defined compared to those after HIP cycle C (Fig. 8(c)). This is an indication that HIP cycle C resulted in better consolidation than HIP cycles A and B.
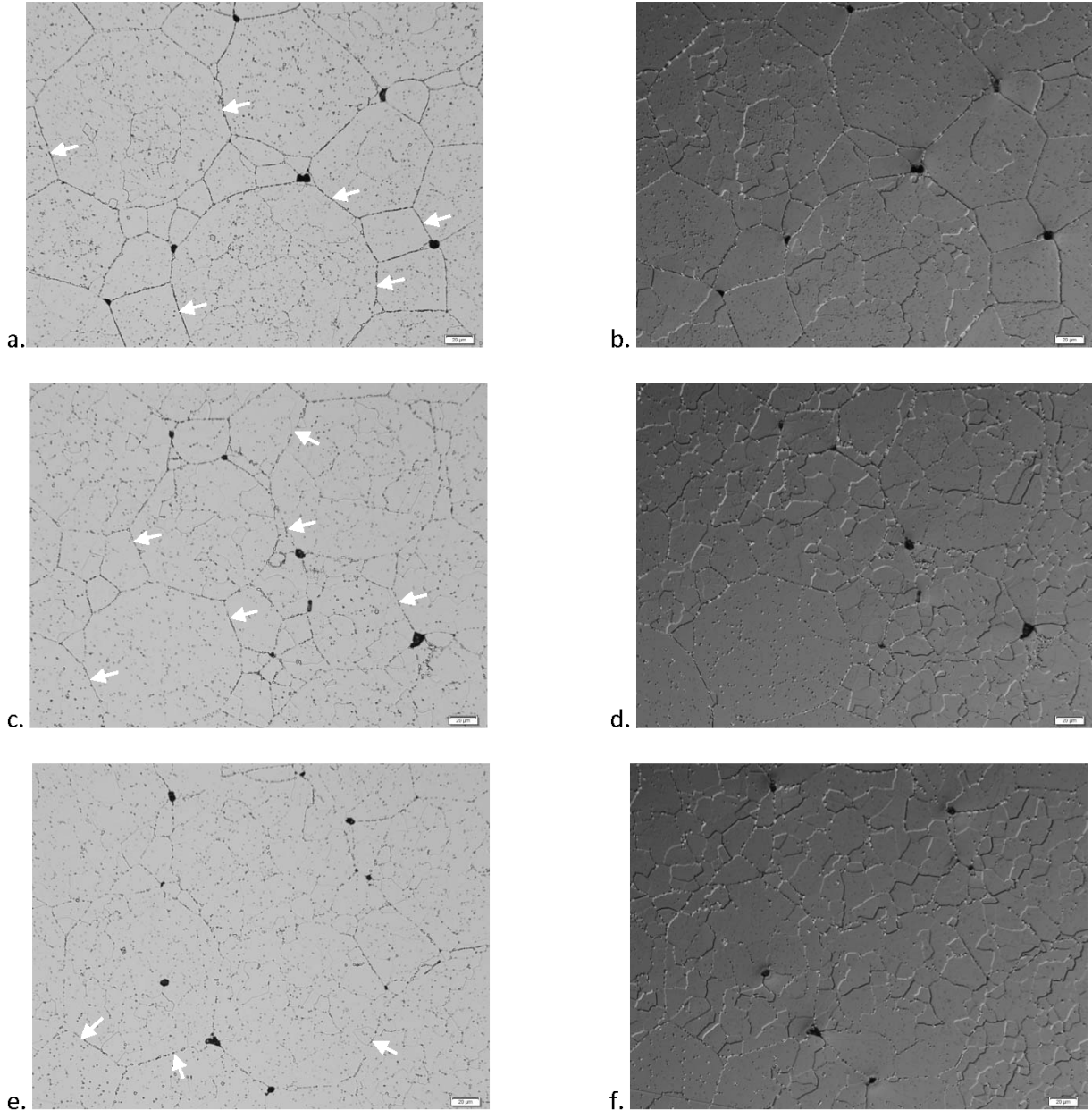


Figure 8.—Brightfield (left column) and differential interference contrast (right column) optical photomicrographs of heat treated material after 2 h HIP cycles A (a-b), B (c-d) and C (e-f). Specimens were swab-etched for approximately 90 sec with a room temperature aqueous solution of 1vol.%Hf and 10vol.%$HNO_3$. Several prior particle boundaries are indicated with arrows.

Figure 9 shows the microstructure of the material after the 20-h HIP cycles D, E, and F. Clearly, the number of pores are markedly reduced. Also, after HIP cycles E and F, the grains are noticeably larger as a result of grain growth during the longer HIP cycles at 1000 °C. There is only a slight indication of prior particle boundaries after HIP cycles E and F compared to the microstructure after HIP cycle D. Table 4 lists the grain size measurements for each of the heat treated specimens along with their hardness values. The grain sizes are calculated based on the average number of grains per square millimeter, as recommended in the standard procedure (Ref. 20).
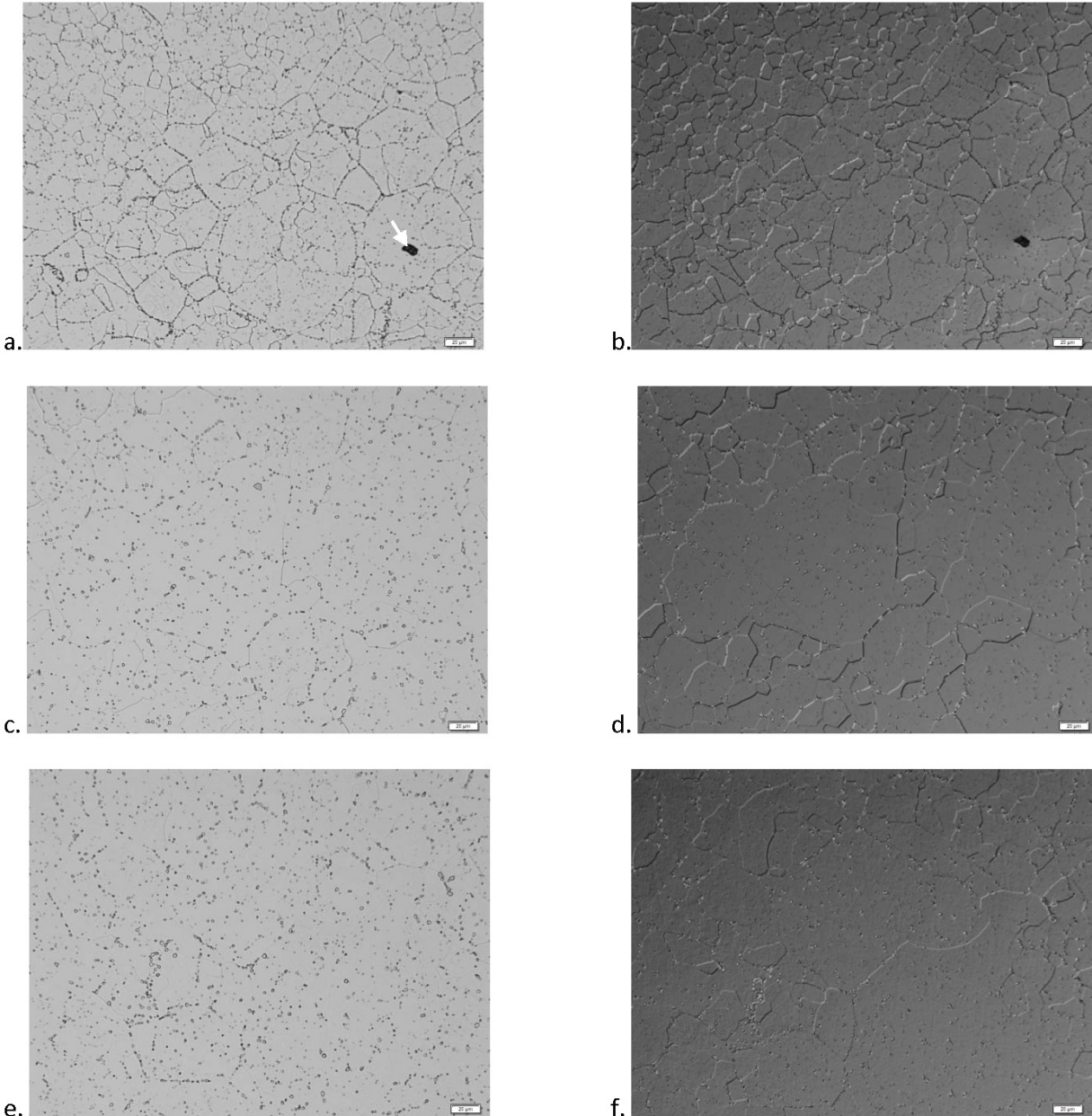


Figure 9.—Brightfield (left column) and differential interference contrast (right column) optical photomicrographs of heat treated material after 20 h HIP cycles D (a-b), E (c-d) and F (e-f). Specimens swab-etched for approximately 90 sec with a room temperature aqueous solution of 1vol.%Hf and 10vol.%HNO₃. A pore that has resulted from trapped gas is indicated with an arrow in Figure 9(a). Prior particle boundaries are nondistinct in 8(c) to (f).

TABLE 4.—GRAIN SIZE RESULTS

| HIP condition | Grains/mm$^2$ | Grain diameter μm | Hardness HV |
|---|---|---|---|
| A | 1067±121 | 31 | 701.4±2.5 |
| B | 1340±123 | 27 | 689.9±8.3 |
| C | 1321±209 | 28 | 720.3±11 |
| D | 1282±81 | 28 | 706.0±4.7 |
| E | 881±104 | 34 | 711.6±4.3 |
| F | 898±41 | 33 | 708.8±4.4 |
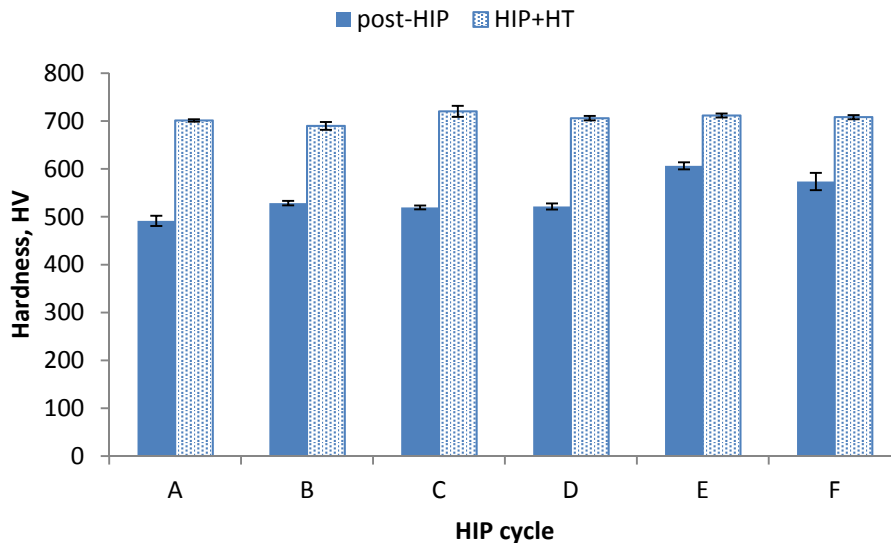


Figure 10.—Average microindentation hardness of 60-Nitinol HIP specimens before and after 1050 °C heat treatment.

Microindentation hardness of the material following HIP processing and following heat treatment is shown in Figure 10. The relative standard error (i.e., the standard deviation divided by the average) for each of the hardness measurements was typically within 1 percent, indicating good precision in the data. An analysis of variation for these data (provided in the Appendix) indicated that there was a statistically significant difference in hardness with respect to the various specimen treatments. A pairwise multiple comparison showed specific cases where the difference in mean hardness values were statistically significant (e.g., cycle A vs. cycle B and cycles B vs. C). Therefore, the heat treated material consolidated with HIP cycle C had the highest hardness (approximately 720 HV) with a confidence level of 95 percent.

The increase in hardness due to heat treatment decreased from HIP cycle A through cycle F. For example, heat treatment after HIP cycles A through D increase hardness approximately 30 to 40 percent. However, heat treatment after HIP cycles E and F only increase hardness approximately 20 percent. This indicates that some solutionizing was occurring during extended HIP cycles. This benefit could be obtained at a lower cost with a homogenization treatment after HIP. This material is typically homogenized at 1050 °C for 48 h followed by furnace cooling (Ref. 24).

Displayed graphically in Figure 11, the volume fraction of parent phase NiTi increased from HIP cycles A through F, though it was essentially constant for cycles B, C and D, within the reported standard deviation. The increase in the fraction of parent phase, and the attendant decrease of precipitate phases was an indication that an increased percentage of second phases had gone into solid solution prior to heat treatment. This result corroborates the result discussed above where it appears that more material went into solid solution as the HIP cycle duration was extended.
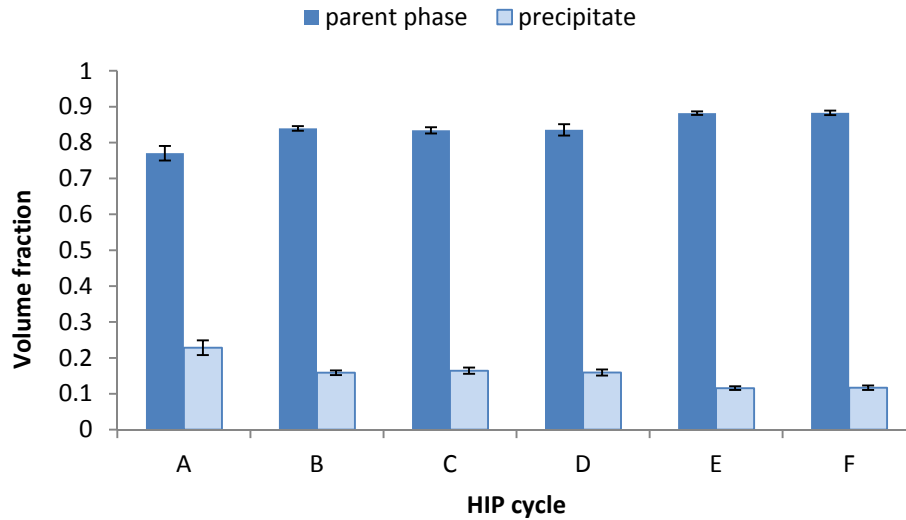
Figure 11.—Average volume fraction of HIP specimens with parent phase (NiTi) and precipitate phase ($Ni_3Ti$) after heat treatment.
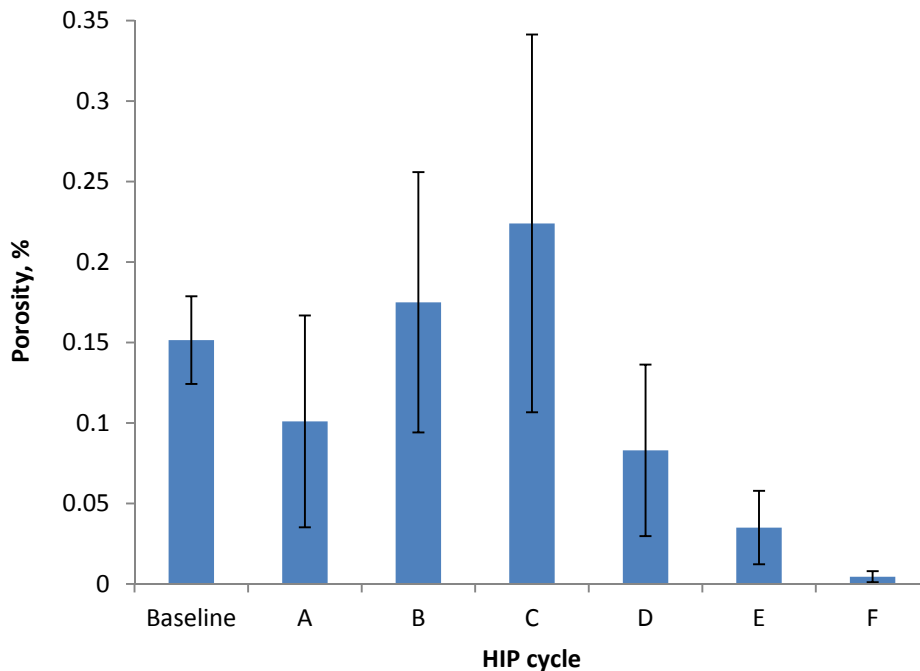


Figure 12.—Measured porosity in each HIP specimen after heat treatment.

As shown in Figure 12, the average porosity increased slightly from HIP cycle A to C, and then decreased monotonically for cycles D to F. Due to the fact that the porosity was low and well dispersed, the data had high relative standard error. A pairwise multiple comparison (Appendix) indicated that the differences between all pairs of mean porosity values were statistically significant, except for the means from HIP cycles B and C. Therefore the increase in porosity from HIP cycle A to HIP cycles B and C is statistically significant. Although porosity is lower after the longer (20 h) HIP cycles, the costs associated with extended operation of HIP units would make this option cost prohibitive for most users.

The porosity measurement technique used in this study did not account for the shape, size or distribution of the pores. Therefore, a group of small, well-dispersed, spherically-shape pores could occupy the same volume as fewer, larger, more angular pores. The latter scenario, however, clearly poses more potential for fracture initiation. A similar situation is illustrated in Figure 13 where the pores that remain after HIP cycle A are larger and more angular than those remaining after HIP cycle C. The more angular pores in Figure 13(a) are more likely to initiate fracture because the acute angles tend to act as stress concentrators. The more rounded pore shape (along with the reduced prior particle boundaries discussed previously) indicates more complete consolidation (Ref. 5). Therefore, although the measured porosity from treatment A was lower than treatments B or C, the shape of the pores after treatment C indicate that this treatment will result in better mechanical properties. It should be noted that the porosity values resulting from each of the studied treatments were relatively low (less than 0.5 percent for all treatments) and comparable to the baseline (0.15 percent porosity). This suggests that, when porosity alone is used as an indicator, the consolidation of 60-Nitinol is fairly robust over the studied range of HIP cycles.
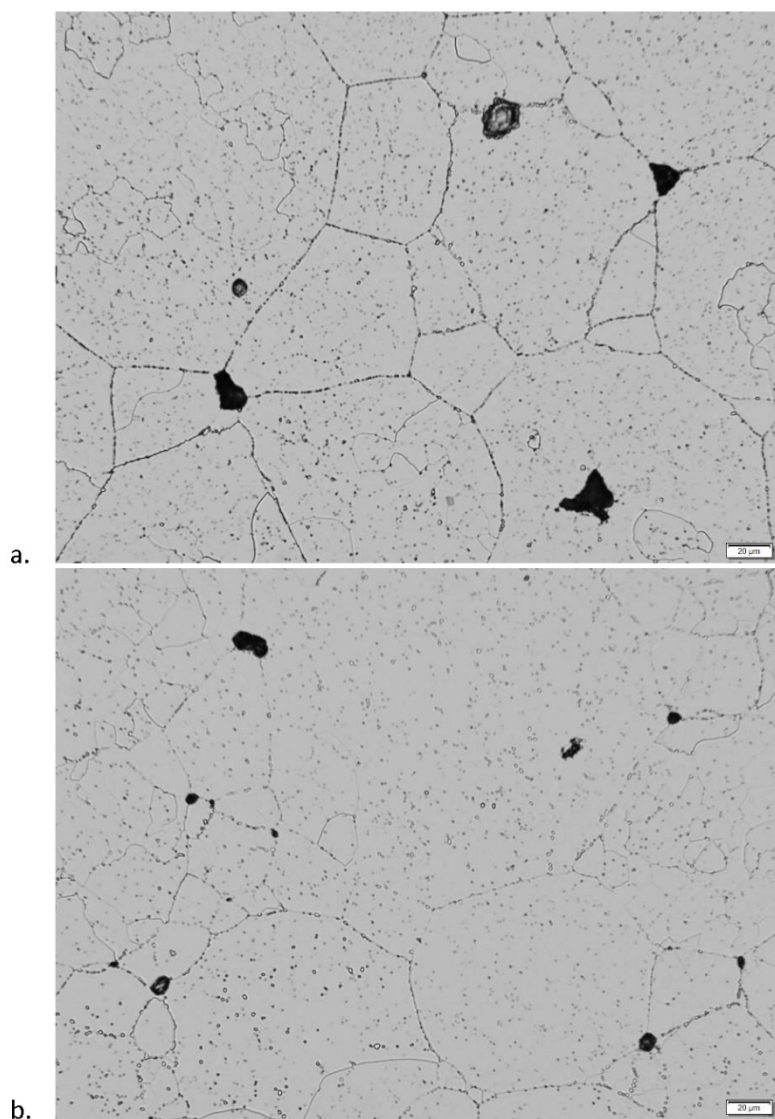


Figure 13.—Optical photomicrograph of specimens after (a) HIP cycle A and (b) HIP cycle C. The pores in *a*, like those in the baseline material (Fig. 3), are generally more angular than those in *b*.

# Summary and Conclusion

The consolidation of gas atomized 60-Nitinol (60wt%Ni – 40wt%Ti) by hot isostatic pressing (HIP) using several different combinations of time, temperature and pressure was studied. Based on the results of this study, the following can be said:

- HIP cycle C (2 h at 1000 °C and 200 MPa), yielded material with the highest hardness (720.3±11 HV).
- Compared to the 2-hr HIP cycles (HIP cycles A through C), porosity decreased after the 20 h HIP cycles (HIP cycles D through F).
- Average grain size was highest after the extended duration (20 h) HIP cycles at 1000 °C and lowest after the 2 h HIP cycle at 100 MPa.

Based on the fact that the highest hardness was obtained using HIP cycle C (2 h/1000 °C/200 MPa), as well as the indications of better consolidation discussed previously, this HIP cycle should be considered for future 60-Nitinol fabrication.

Inclusion of larger particles (e.g., 300 μm) should be studied in the future. This would reduce the total surface area of the powder, thereby reducing the affinity for adsorption of oxygen (thereby minimizing oxide films). Widening the particle size distribution would also increase the packing factor of the powder, possibly reducing porosity (Refs. 25 and 26). However, if larger particles introduce more porosity due to trapped internal gas, the desired effect could offset. Moreover, the effect of increasing the particle size distribution on powder handling would need to be investigated due to the likely increase this would have on interparticle friction.

It is anticipated that the results of this study will be used to assist future commercial development of this material, especially for HIP processing and near net-shape product design.

# Appendix

The results of statistical analyses of the hardness data, comparing the hardness of as-HIPped specimens to those that were heat treated by water-quenching from 1050 °C. An excellent explanation of the statistical techniques used here has been provided by George P. Box, J. Stuart Hunter and William G. Hunter in "Statistics for Experimenters: Design, Innovation, and Discovery," 2nd ed., John Wiley & Sons, 2005.

**One Way Repeated Measures Analysis of Variance**
Hardness of as-HIPped (AH) and water quenched (WQ) specimens treated with HIP cycles A through F
**Normality Test:** Failed (P < 0.050)
**Equal Variance Test:** Passed (P = 0.071)

| Treatment Name | N | Missing | Mean | Std Dev | SEM |
|---|---|---|---|---|---|
| C/AH | 6 | 0 | 519.574 | 3.914 | 1.598 |
| B/AH | 6 | 0 | 528.507 | 4.764 | 1.945 |
| A/AH | 6 | 0 | 491.503 | 10.619 | 4.335 |
| D/AH | 7 | 0 | 521.549 | 6.294 | 2.379 |
| F/AH | 7 | 0 | 573.614 | 16.747 | 6.330 |
| E/AH | 7 | 0 | 606.439 | 7.325 | 2.769 |
| C/WQ | 7 | 1 | 719.893 | 15.005 | 6.126 |
| B/WQ | 7 | 0 | 689.931 | 8.285 | 3.131 |
| A/WQ | 6 | 0 | 701.356 | 2.527 | 1.032 |
| D/WQ | 7 | 0 | 706.019 | 4.699 | 1.776 |
| F/WQ | 6 | 0 | 709.055 | 4.381 | 1.789 |
| E/WQ | 7 | 0 | 711.638 | 4.302 | 1.626 |

| Source of Variation | DF | SS | MS | F | P |
|---|---|---|---|---|---|
| Between Subjects | 6 | 116.931 | 19.489 | | |
| Between Treatments | 11 | 579644.203 | 52694.928 | 660.300 | <0.001 |
| Residual | 60 | 4788.273 | 79.805 | | |
| Total | 77 | 589546.344 | 7656.446 | | |

The differences in the mean values among the treatment groups are greater than would be expected by chance; there is a statistically significant difference (P = <0.001). To isolate the group or groups that differ from the others, a multiple comparison procedure was performed (results follow).

Power of performed test with alpha = 0.050: 1.000

Expected Mean Squares:
Approximate DF Residual = 60.000
Expected MS(Subj) = var(res) + 11.000 var(Subj)
Expected MS(Treatment) = var(res) + var(Treatment)
Expected MS(Residual) = var(res)

All Pairwise Multiple Comparison Procedures (Student-Newman-Keuls Method):
Comparisons for factor:

| Comparison | Diff of Means | p | q | P | P<0.050 |
|---|---|---|---|---|---|
| C/WQ vs. A/AH | 228.335 | 12 | 62.087 | <0.001 | Yes |
| C/WQ vs. C/AH | 200.264 | 11 | 54.454 | <0.001 | Yes |
| C/WQ vs. D/AH | 198.539 | 10 | 56.293 | <0.001 | Yes |
| C/WQ vs. B/AH | 191.330 | 9 | 52.025 | <0.001 | Yes |
| C/WQ vs. F/AH | 146.474 | 8 | 41.531 | <0.001 | Yes |
| C/WQ vs. E/AH | 113.648 | 7 | 32.223 | <0.001 | Yes |
| C/WQ vs. B/WQ | 30.157 | 6 | 8.551 | <0.001 | Yes |
| C/WQ vs. A/WQ | 18.481 | 5 | 5.025 | 0.007 | Yes |
| C/WQ vs. D/WQ | 14.068 | 4 | 3.989 | 0.032 | Yes |
| C/WQ vs. F/WQ | 10.783 | 3 | 2.932 | 0.104 | No |
| C/WQ vs. E/WQ | 8.450 | 2 | 2.396 | 0.096 | Do Not Test |
| E/WQ vs. A/AH | 219.885 | 11 | 62.225 | <0.001 | Yes |
| E/WQ vs. C/AH | 191.814 | 10 | 54.281 | <0.001 | Yes |
| E/WQ vs. D/AH | 190.089 | 9 | 56.298 | <0.001 | Yes |
| E/WQ vs. B/AH | 182.880 | 8 | 51.753 | <0.001 | Yes |
| E/WQ vs. F/AH | 138.024 | 7 | 40.878 | <0.001 | Yes |
| E/WQ vs. E/AH | 105.198 | 6 | 31.156 | <0.001 | Yes |
| E/WQ vs. B/WQ | 21.707 | 5 | 6.429 | <0.001 | Yes |
| E/WQ vs. A/WQ | 10.031 | 4 | 2.839 | 0.197 | No |
| E/WQ vs. D/WQ | 5.619 | 3 | 1.664 | 0.472 | Do Not Test |
| E/WQ vs. F/WQ | 2.333 | 2 | 0.660 | 0.642 | Do Not Test |
| F/WQ vs. A/AH | 217.552 | 10 | 59.050 | <0.001 | Yes |
| F/WQ vs. C/AH | 189.481 | 9 | 51.431 | <0.001 | Yes |
| F/WQ vs. D/AH | 187.756 | 8 | 53.133 | <0.001 | Yes |
| F/WQ vs. B/AH | 180.547 | 7 | 49.006 | <0.001 | Yes |
| F/WQ vs. F/AH | 135.691 | 6 | 38.399 | <0.001 | Yes |
| F/WQ vs. E/AH | 102.866 | 5 | 29.110 | <0.001 | Yes |
| F/WQ vs. B/WQ | 19.374 | 4 | 5.483 | 0.002 | Yes |
| F/WQ vs. A/WQ | 7.699 | 3 | 2.090 | 0.309 | Do Not Test |
| F/WQ vs. D/WQ | 3.286 | 2 | 0.930 | 0.514 | Do Not Test |
| D/WQ vs. A/AH | 214.266 | 9 | 60.635 | <0.001 | Yes |
| D/WQ vs. C/AH | 186.195 | 8 | 52.691 | <0.001 | Yes |
| D/WQ vs. D/AH | 184.471 | 7 | 54.634 | <0.001 | Yes |
| D/WQ vs. B/AH | 177.262 | 6 | 50.163 | <0.001 | Yes |
| D/WQ vs. F/AH | 132.406 | 5 | 39.214 | <0.001 | Yes |
| D/WQ vs. E/AH | 99.580 | 4 | 29.492 | <0.001 | Yes |
| D/WQ vs. B/WQ | 16.089 | 3 | 4.765 | 0.004 | Yes |
| D/WQ vs. A/WQ | 4.413 | 2 | 1.249 | 0.381 | Do Not Test |
| A/WQ vs. A/AH | 209.853 | 8 | 56.960 | <0.001 | Yes |
| A/WQ vs. C/AH | 181.783 | 7 | 49.341 | <0.001 | Yes |
| A/WQ vs. D/AH | 180.058 | 6 | 50.954 | <0.001 | Yes |
| A/WQ vs. B/AH | 172.849 | 5 | 46.916 | <0.001 | Yes |
| A/WQ vs. F/AH | 127.993 | 4 | 36.221 | <0.001 | Yes |
| A/WQ vs. E/AH | 95.167 | 3 | 26.931 | <0.001 | Yes |
| A/WQ vs. B/WQ | 11.676 | 2 | 3.304 | 0.023 | Yes |
| B/WQ vs. A/AH | 198.178 | 7 | 56.082 | <0.001 | Yes |
| B/WQ vs. C/AH | 170.107 | 6 | 48.138 | <0.001 | Yes |
| B/WQ vs. D/AH | 168.382 | 5 | 49.869 | <0.001 | Yes |

| | | | | | |
|---|---|---|---|---|---|
| B/WQ vs. B/AH | 161.173 | 4 | 45.610 | <0.001 | Yes |
| B/WQ vs. F/AH | 116.317 | 3 | 34.449 | <0.001 | Yes |
| B/WQ vs. E/AH | 83.491 | 2 | 24.727 | <0.001 | Yes |
| E/AH vs. A/AH | 114.686 | 6 | 32.455 | <0.001 | Yes |
| E/AH vs. C/AH | 86.615 | 5 | 24.511 | <0.001 | Yes |
| E/AH vs. D/AH | 84.891 | 4 | 25.142 | <0.001 | Yes |
| E/AH vs. B/AH | 77.682 | 3 | 21.983 | <0.001 | Yes |
| E/AH vs. F/AH | 32.826 | 2 | 9.722 | <0.001 | Yes |
| F/AH vs. A/AH | 81.861 | 5 | 23.166 | <0.001 | Yes |
| F/AH vs. C/AH | 53.790 | 4 | 15.222 | <0.001 | Yes |
| F/AH vs. D/AH | 52.065 | 3 | 15.420 | <0.001 | Yes |
| F/AH vs. B/AH | 44.856 | 2 | 12.694 | <0.001 | Yes |
| B/AH vs. A/AH | 37.005 | 4 | 10.044 | <0.001 | Yes |
| B/AH vs. C/AH | 8.934 | 3 | 2.425 | 0.208 | No |
| B/AH vs. D/AH | 7.209 | 2 | 2.040 | 0.154 | Do Not Test |
| D/AH vs. A/AH | 29.796 | 3 | 8.432 | <0.001 | Yes |
| D/AH vs. C/AH | 1.725 | 2 | 0.488 | 0.731 | Do Not Test |
| C/AH vs. A/AH | 28.071 | 2 | 7.619 | <0.001 | Yes |

**One Way Repeated Measures Analysis of Variance**
Hardness of water quenched (WQ) specimens treated with HIP cycles A through F
**Normality Test:**     Failed   (P < 0.050)
**Equal Variance Test:**  Passed  (P = 0.168)

| Treatment Name | N | Missing | Mean | Std Dev | SEM |
|---|---|---|---|---|---|
| C/WQ | 7 | 1 | 719.893 | 15.005 | 6.126 |
| B/WQ | 7 | 0 | 689.931 | 8.285 | 3.131 |
| A/WQ | 6 | 0 | 701.356 | 2.527 | 1.032 |
| D/WQ | 7 | 0 | 706.019 | 4.699 | 1.776 |
| F/WQ | 6 | 0 | 709.055 | 4.381 | 1.789 |
| E/WQ | 7 | 0 | 711.638 | 4.302 | 1.626 |

| Source of Variation | DF | SS | MS | F | P |
|---|---|---|---|---|---|
| Between Subjects | 6 | 404.603 | 67.434 | | |
| Between Treatments | 5 | 3467.814 | 693.563 | 12.447 | <0.001 |
| Residual | 27 | 1504.439 | 55.720 | | |
| Total | 38 | 5282.592 | 139.016 | | |

The differences in the mean values among the treatment groups are greater than would be expected by chance; there is a statistically significant difference (P = <0.001). To isolate the group or groups that differ from the others, a multiple comparison procedure was performed (results follow).

Power of performed test with alpha = 0.050: 1.000

Expected Mean Squares:
Approximate DF Residual = 27.000
Expected MS(Subj) = var(res) + 5.500 var(Subj)
Expected MS(Treatment) = var(res) + var(Treatment)
Expected MS(Residual) = var(res)

All Pairwise Multiple Comparison Procedures (Student-Newman-Keuls Method):

Comparisons for factor:

| Comparison | Diff of Means | p | q | P | P<0.050 |
|---|---|---|---|---|---|
| C/WQ vs. B/WQ | 30.710 | 6 | 10.377 | <0.001 | Yes |
| C/WQ vs. A/WQ | 19.545 | 5 | 6.312 | 0.001 | Yes |
| C/WQ vs. D/WQ | 14.622 | 4 | 4.941 | 0.009 | Yes |
| C/WQ vs. F/WQ | 11.846 | 3 | 3.826 | 0.031 | Yes |
| C/WQ vs. B/WQ | 9.003 | 2 | 3.042 | 0.041 | Yes |
| E/WQ vs. B/WQ | 21.707 | 5 | 7.694 | <0.001 | Yes |
| E/WQ vs. A/WQ | 10.541 | 4 | 3.555 | 0.080 | No |
| E/WQ vs. D/WQ | 5.619 | 3 | 1.991 | 0.351 | Do Not Test |
| E/WQ vs. F/WQ | 2.843 | 2 | 0.959 | 0.504 | Do Not Test |
| F/WQ vs. B/WQ | 18.864 | 4 | 6.363 | <0.001 | Yes |
| F/WQ vs. A/WQ | 7.699 | 3 | 2.482 | 0.204 | Do Not Test |
| F/WQ vs. D/WQ | 2.776 | 2 | 0.936 | 0.514 | Do Not Test |
| D/WQ vs. B/WQ | 16.089 | 3 | 5.702 | 0.001 | Yes |
| D/WQ vs. A/WQ | 4.923 | 2 | 1.660 | 0.251 | Do Not Test |
| A/WQ vs. B/WQ | 11.166 | 2 | 3.766 | 0.013 | Yes |

A result of "Do Not Test" occurs for a comparison when no significant difference is found between two means that enclose that comparison. For example, if you had four means sorted in order, and found no difference between means 4 vs. 2, then you would not test 4 vs. 3 and 3 vs. 2, but still test 4 vs. 1 and 3 vs. 1 (4 vs. 3 and 3 vs. 2 are enclosed by 4 vs. 2: 4 3 2 1). Note that not testing the enclosed means is a procedural rule, and a result of Do Not Test should be treated as if there is no significant difference between the means, even though one may appear to exist.

# References

1. W.J. Buehler, "Intermetallic Compound Based Materials for Structural Applications," in The Seventh Navy Science Symposium: Solution to Navy Problems Through Advanced Technology, May 14, 15, 16, 1963, U.S. Naval Aviation Medical Center, Pensacola, Florida. Vol. 1, Office of Naval Research, Arlington, VA, 16 May 1963.
2. W.J. Buehler and F.E. Wang, "A Summary of Recent Research on the Nitinol Alloys and their Potential Application in Ocean Engineering," Ocean Engineering, Vol. 1, pp. 105-120, 1968.
3. C. DellaCorte, S.V. Pepper, R. Noebe, D.R. Hull, G. Glennon, "Intermetallic Nickel-Titanium Alloys for Oil-Lubricated Bearing Applications," NASA/TM—2009-215646, March 2009, National Technical Information Service, Springfield, VA.
4. C. DellaCorte, R. Noebe, M.K. Stanford and S.A. Padula, "Resilient and Corrosion-Proof Rolling Element Bearings Made From Superelastic Ni-Ti Alloys for Aerospace Mechanism Applications," NASA/TM—2011-217105, National Technical Information Service, Springfield, VA.
5. R.M. German, Powder Metallurgy & Particulate Materials Processing, 2005, Metal Powder Industries Federation, Princeton, NJ.
6. M.K. Stanford, "Charpy Impact Energy and Microindentation Hardness of 60-Nitinol," NASA/TM—2012-216029, NASA Center for Technical Information, Hanover, MD, 2012.
7. M.K. Stanford, F. Thomas and C. DellaCorte, "Processing Issues for Preliminary Melts of the Intermetallic Compound 60-NITINOL, NASA/TM—2012-216044, NASA Center for Technical Information, Hanover, MD, 2012.
8. ASTM Designation E 1447 – 09, "Standard Test Method for Determination of Hydrogen in Titanium and Titanium Alloys by the Inert Gas Fusion Thermal Conductivity/Infrared Detection Method," 2015, vol. 03.05, American Society for Testing and Materials, West Conshokocken, PA.
9. ASTM Designation E 1941 – 10, "Standard Test Method for Determination of Carbon in Refractory and Reactive Metals and Their Alloys by Combustion Analysis," 2015, vol. 03.05, American Society for Testing and Materials, West Conshokocken, PA.
10. ASTM Designation B822 – 10, "Standard Test Method for Particle Size Distribution of Metal Powders and Related Compounds by Light Scattering," 2011, vol. 02.05, American Society for Testing and Materials, West Conshokocken, PA.
11. ASTM Test Method B 212-99. 2001. Standard Test Method for Determination of Apparent Density of Free-Flowing Metal Powders Using the Hall Flowmeter Funnel. Annual Book of ASTM Standards, Vol. 02.05. West Conshohocken, PA: American Society for the Testing of Metals.
12. ASTM Test Method B 527-93(2001)$^{\varepsilon 1}$. 2001. Standard Test Method for Determination of Tap Density of Metallic Powders and Compounds. Annual Book of ASTM Standards, Vol. 02.05. West Conshohocken, PA: American Society for the Testing of Metals.
13. ASTM Test Method B 213-97. 1998. Standard Test Method for Flow Rate of Metal Powders. Annual Book of ASTM Standards, Vol. 02.05. West Conshohocken, PA: American Society for the Testing of Metals.
14. E. Klar and W.M. Shafer, "High-Pressure Gas Atomization of Metals," in Powder Metallurgy for High Performance Applications, John J. Burke and Volker Weiss eds., pp. 57-68, Syracuse University Press, New York, 1972.
15. J.K. Beddow, The Production of Metal Powders by Atomization, Heyden, London, 1978.
16. J.J. Dunkley, "Atomization," in ASM Handbook, Vol. 7, Powder Metal Technologies and Applications, ASM International, Materials Park, Ohio, 1998.
17. ASTM Test Method B 923-10. 2014. Standard Test Method for Metal Powder Skeletal Density by Helium or Nitrogen Pycnometry. Annual Book of ASTM Standards, Vol. 02.05. West Conshohocken, PA: American Society for the Testing of Metals.
18. ASTM Test Method E 3-11. 2014. Standard Guide for Preparation of Metallographic Specimens. Annual Book of ASTM Standards, Vol. 03.01. West Conshohocken, PA: American Society for the Testing of Metals.

19. ASTM Test Method E 384-11$^{\varepsilon 1}$. 2011. Standard Test Method for Knoop and Vickers Hardness of Materials. Annual Book of ASTM Standards, Vol. 03.01. West Conshohocken, PA: American Society for the Testing of Metals.
20. ASTM Test Method E 112-10. 2001. Standard Test Method for Determining Average Grain Size. Annual Book of ASTM Standards, Vol. 03.01. West Conshohocken, PA: American Society for the Testing of Metals.
21. M.K. Stanford, Ph.D. thesis, University of Dayton, 2002.
22. E.C. Abdullah and D. Geldart, The Use of Bulk Density Measurements as Flowability Indicators, Powder Technology, Vol. 102, pp. 151-165, 1999.
23. R.O. Grey and J.K. Beddow, On the Hausner Ratio and its Relationship to Some Properties on Metal Powders, Powder Technology, Vol. 2, pp. 323-326, 1969.
24. M.K. Stanford, "Hardness and Microstructure of Binary and Ternary Nitinol Compounds," to be published as a NASA Technical Memorandum.
25. R.N. German, "Particle Packing Characteristics," Metal Powder Industries Federation, New Jersey, 1989.
26. D.J. Cumberland and R.J. Crawford, "The Packing of Particles," Elsevier, Amsterdam, 1987.